Journal of Physical Chemistry & Biophysics
ISSN: 2161-0398

Sahbeni et al., J Phys Chem Biophys 2017, 7:3
DOI: 10.4172/2161-0398.1000257

Research Article Open Access

Annealing Temperature Effect on the Physical Properties of Titanium Oxide Thin Films Prepared by the Sol-Gel Method

Sahbeni K[1,2,6]*, Sta I[2,3], Jlassi M[3,4], Kandyla M[6], Hajji M[3,5], Kompitsas M[6] and Dimassi W[1]

[1]Laboratoire Photovoltaïque, Centre de Recherche et des Technologies de l'Energie, Technopole de Borj-Cedria, BP 95, 2050, Hammam-Lif, Tunisia
[2]Faculté des sciences de Bizerte, 7021 Jarzouna, Tunisia
[3]Laboratoire de Semi-conducteur, Nano-structure et Technologie Avancée, Centre de Recherche et des Technologies de l'Energie, Technopole de Borj-Cedria, BP 95, 2050, Hammam-Lif, Tunisia
[4]Ecole Supérieure des Sciences et Technologies du Design. Université de la Manouba, P5, Den Den, Tunisia
[5]Ecole Nationale d'Electronique des Communication de Sfax, Technopôle de Sfax, Route de Tunis Km 10, Cité El Ons, BP 1163, 3021, Sfax, Tunisia
[6]National Hellenic Research Foundation, Theoretical and Physical Chemistry Institute, 48, Vasileos Constantinou Ave., 11635 Athens, Greece

Abstract

In this work, the low-cost sol–gel, spin-coating technique was used to grow TiO2 thin films on silicon substrates. The influence of annealing temperature on the structural, morphological, and optical properties of TiO2 films is investigated. The structural properties of the TiO2 films are investigated by Raman and Fourier transform infrared (FTIR) Spectroscopy. Morphological properties are studied by Atomic Force Microscopy (AFM). The optical properties are examined by photoluminescence (PL) and ultraviolet-visible (UV-vis) spectroscopy.

Keywords: Thin films; Titanium oxide; Sol-gel; Annealing temperature; Physical properties

Introduction

Titanium finds more and more applications today. Over 96% of the world-wide use of titanium is in its oxide form, TiO_2 (titanium dioxide), thus creating a high demand for this material, due to a wide range of potential applications for environmental purposes [1]. It is extensively used for photo degradation of organic and inorganic pollutants [2], photovoltaic energy production [3], hydrogen production by water photo-splitting [4,5], and gas sensing [6,7]. This variety of applications is because of TiO_2 low cost, non-toxicity, as well as useful optical, physical, chemical, and electronic properties, including excellent transmittance of visible light, photo catalytic behavior, high dielectric constant, high refractive index, and high chemical stability [8,9].

It is well known that TiO_2 is an n-type semiconductor with an indirect energy band gap [6,10,11]. It generally crystallizes in three phases, the tetrahedral anatase (space group $I4_1/amd$, density=3.894 g/cm^2), rutile (space group $P4_2/mnm$, density=4.25 g/cm^2) and orthorhombic brookite (space group Pcab, density=4.12 g/cm^2). The anatase and rutile phases belong to different space groups but both have a tetragonal crystal lattice. Rutile is the most stable form of TiO_2, whereas anatase and brookite are metastable and transform to the rutile phase upon heating [6,12-14]. Conventional methods to prepare TiO_2 thin films are pulsed laser deposition (PLD) [15,16], RF magnetron sputtering [17-19] plasma enhanced chemical vapor deposition [20], and sol-gel methods [6,15,21,22], among others. Focusing on the sol-gel method, it is one of the most attractive techniques for thin-film deposition, because of low cost, non-vacuum requirements, large area deposition, and low temperature processing. Furthermore, the sol-gel method produces thin films which have good homogeneity, excellent compositional control, and good electrical and optical properties [23].

The effect of the annealing temperature on TiO_2 powders has been often reported in the literature [11-13]. Mathpal et al. have studied the effect of annealing temperature on the structural and luminescence properties of TiO_2 powders [12]. Another study has investigated the effect of the annealing temperature on TiO_2 thin films, prepared by the sol-gel method and dip-coating techniques [22]. These studies have that the annealing temperature influences the structural and optical properties of TiO_2 thin films. Fewer articles investigate the phase transition (from anatase to rutile) of TiO_2 thin films obtained by the sol-gel and spin coating techniques with annealing temperature, as most articles study the properties of these films at lower temperatures [6].

Hence, we performed this work to understand the physical properties of TiO_2 sol-gel more systemically and deeply. The TiO_2 thin films are prepared by the sol-gel spin coating method and annealed between 40 and 900°C. The variation of structural properties of the thin film was studied through Raman, FTIR, PL spectroscopy and AFM microscopy. The crystalline structure, surface morphology and optical properties of the TiO_2 thin film were then studied and discussed. All results indicate the dependence of the formed phases (anatase, rutile, or mixed anatase-rutile phase) of TiO_2 thin films on the annealing temperature and indicate a phase transition which starts at 600°C. This simple and no toxic method provided us results similar to those given by other method more difficult and requires hard realization conditions, in one hand. In other hand, we have shown that TiO_2 thin films deposed in silicon substrates is a good agent to produce antireflecting coating for solar cells.

Experimental

The precursor solutions of TiO_2, prepared by the sol-gel method, were obtained using titanium (IV) isopropoxide ($C_{12}H_{28}O_4Ti$) as the starting material. The titanium (IV) isopropoxide was initially added in a mixture of ethanol and monoethanolamine (MEA) and the

***Corresponding author:** Sahbeni K, National Hellenic Research Foundation, Theoretical and Physical Chemistry Institute, 48, Vasileos Constantinou Ave., 11635 Athens, Greece, Tel: +21698713283; E-mail: sahbani_kaouther@hotmail.fr

Received September 28, 2017; **Accepted** October 08, 2017; **Published** October 14, 2017

Citation: Sahbeni K, Sta I, Jlassi M, Kandyla M, Hajji M, et al. (2017) Annealing Temperature Effect on the Physical Properties of Titanium Oxide Thin Films Prepared by the Sol-Gel Method. J Phys Chem Biophys 7: 257. doi: 10.4172/2161-0398.1000257

concentration of titanium (IV) isopropoxide was 0.5 M. The resultant solution was stirred at 80°C for 1 h to yield a clear and homogeneous solution. In order to prepare TiO_2 thin films, the obtained solution was deposited on silicon substrates by spin coating, with a rate of 3000 rpm for 30 s. The (100) silicon substrates were cleaned with acetone for 10 min, methanol for 10 min, rinsed with deionized (DI) water for 15 min, and then dried with nitrogen. After the spin-coating step, the films were pre-annealed at 300°C for 15 min. Finally, all films were annealed in air at different temperatures in the range of 400 to 900°C for 1 h.

The structural characteristics of the films were investigated by a Raman Jobin Yvon Lab RAM HR spectrometer, using the 632.8 nm irradiation from a He-Ne laser (at 3 mW) and Fourier transform infrared spectroscopy (FTIR). An atomic force microscope (AFM) (Nanoscope III) was used in tapping configuration (Veeco AFM head RTESP silicon pur) to scan an area of 2 μm × 2 μm. The obtained results were used to estimate the surface roughness and the grain size in the film. Standard software was used to calculate the root-mean-square (RMS) roughness and the grain size. The grain size was defined as the diameter of the grain at the middle of the height. Photoluminescence (PL) measurements were performed at room temperature using the fluorescence spectrophotometer (LS 45) with an excitation wavelength of 266 nm. Finally, optical reflectivity spectra were recorded with a Perkin Elmer Lambda 19 spectrophotometer in the 300-1200 nm range.

Results and Discussion

Structural properties

Raman spectra: Figure 1 shows the Raman spectra of TiO_2 thin films produced by the sol-gel method and deposited on silicon substrates, for various annealing temperatures. The spectra exhibit an active mode centered around 665 cm^{-1}, which is attributed to the Eg mode of the anatase phase [12,24]. For all annealing temperatures, Raman scattering reveals the presence of mixed (anatase and rutile) Raman active modes. The 665 cm^{-1} Eg peak position is shifted to higher wavenumbers compared with literature values [24], which indicate a decrease of the particle size [25]. The spectra also exhibit three main phonon modes, B1g, Eg, and Ag, which appear at 140, 433, and 617 cm^{-1}, respectively. This result confirms the presence of a rutile phase TiO_2 [26,27]. The B2g mode of rutile TiO_2 centered at 822 cm^{-1} appears clearly after annealing at 800°C, which shows that the rutile phase becomes gradually the dominant phase starting at 800°C, indicating that the anatase-rutile transition temperature should be less than 800°C. Both phases crystallize in a tetragonal structure [6,12-14]. Two strong peaks at 302 cm^{-1} and 521 cm^{-1} represent the Si-Si stretching mode of the substrate [28]. The peak at 939 cm^{-1} is assigned to the stretching vibrations of Si-OH [29].

FTIR spectra: Figure 2 shows the absorbance spectra of annealed TiO_2 films at different temperatures (from 400-900°C) recorded by

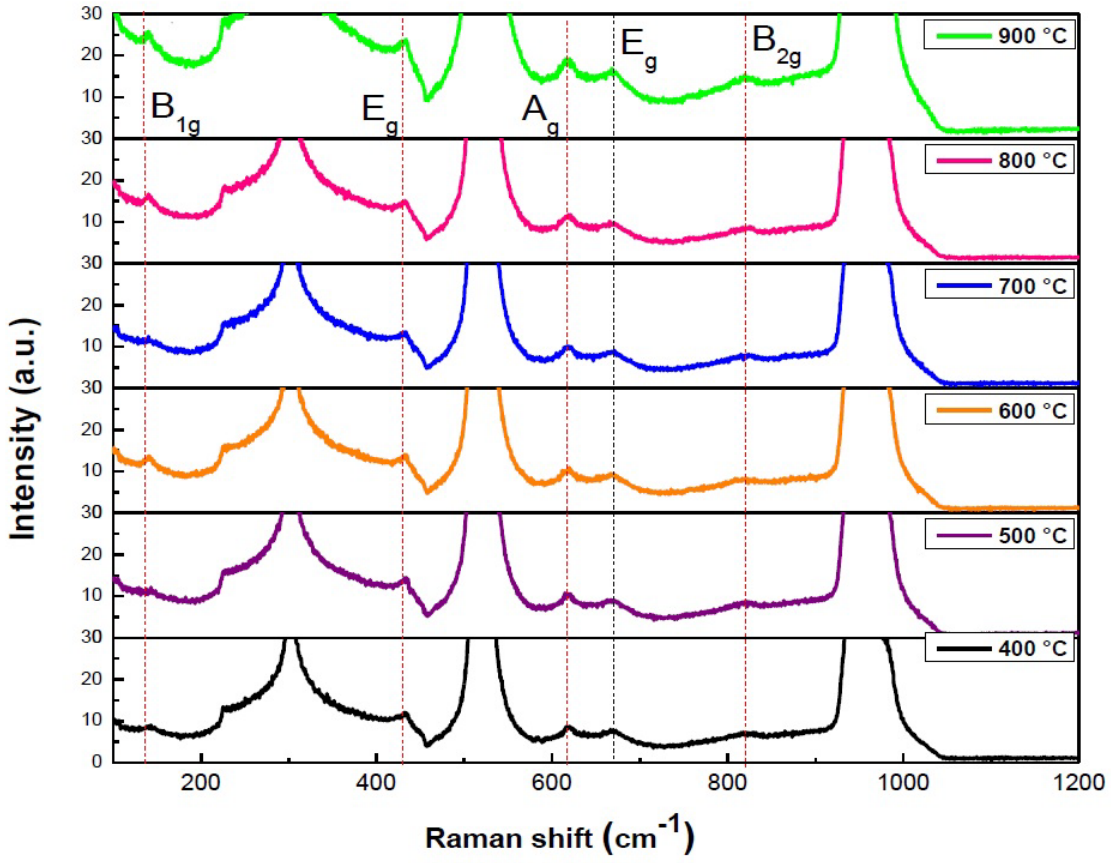

Figure 1: Raman spectra of TiO_2 thin films prepared on silicon substrates, annealed at different temperatures (400°C-900°C).

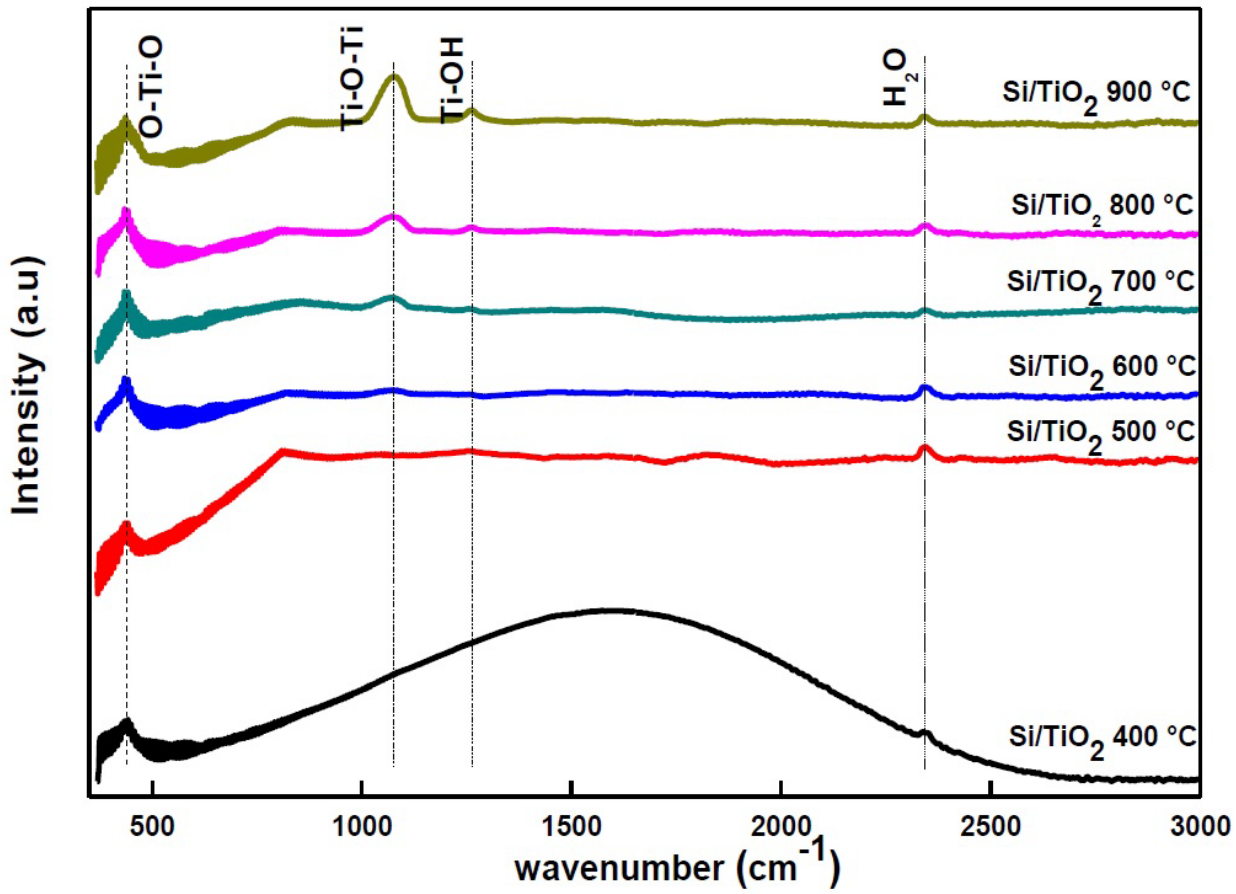

Figure 2: Fourier transform infrared spectra of TiO_2 films annealed at different temperatures (400°C-900°C).

FTIR spectroscopy. The samples annealed at 400°C show a broad hump ranging from 621 nm to 2314 nm, which can be attributed to poor crystallinity and disappears by increasing the annealing temperature. The peak at 2360 cm^{-1} results from adsorbed H_2O molecules, which were not completely removed after sol-gel growth. The peak at 1242 cm^{-1} corresponds to the vibration mode of Ti-OH which is the terminal hydroxyl groups and it's far below the top of the valence band of TiO_2 rutile phase [30,31]. This corresponding band starts to appear at 600°C and his intensity increases by increasing temperature. The peak at 436 cm^{-1} corresponds to the O-Ti-O transverse mode of the anatase TiO_2 phase [32-34]. The band centered at 1072 cm^{-1} appears for the samples treated at 600, 700, 800 and 900°C, and is attributed to Ti-O-Ti vibrations according to rutile phase [31,32]. We find that the intensity of this band increases with increasing annealing temperature. This indicates that the number of Ti-O-Ti vibrations is also growing with increasing annealing temperature.

Morphological properties

To evaluate the surface roughness and the grain size of the TiO_2 films, an area of 2 μm × 2 μm has been scanned by AFM in tapping mode. The two-(2D) and three-dimensional (3D) AFM images for different annealing temperatures are shown in Figures 3a-3c. The sample grains become bigger when the temperature increases from 400°C to 900°C and the surface becomes rougher. The AFM 2D and 3D images show that the temperature affects the density and the size of TiO_2 grains significantly. The grains have been sorted according to their size in order to determine the surface density and grain diameter of the samples. Figures 4a-4c show the obtained histograms of the grain size distribution for three different annealing temperatures. From the AFM images we also find the average RMS roughness values which are 52, 35 and 97 nm for films annealed at 400, 600 and 900°C, respectively (Figure 5). Obviously, a significant increase of the grain size and RMS roughness is observed with the increase of the annealing temperature. This is due to the transformation of TiO_2 from the anatase to the rutile phase, which involves the coalescence of smaller particles into bigger ones [29,35]. The AFM results are in good agreement with the Raman and FTIR findings, which show the dependence of structural changes on thermal annealing: TiO_2 film crystallization is accompanied by densification, as observed on the AFM images.

Optical properties

Photoluminescence: PL spectra of the samples were recorded at room temperature in the wavelength range from 300 to 700 nm (400-700 nm shown in Figure 6). The overall PL intensity increases between 400°C and 500°C. The highest PL intensity for the sample annealed at 500°C is probably due to self-trapped exciton recombination, which is a combined effect of defect centres generated from oxygen vacancies and particle size [12]. For all higher temperatures, the overall PL intensity decreases systematically with annealing temperature, even though a remarkable change of relative PL intensities for the samples

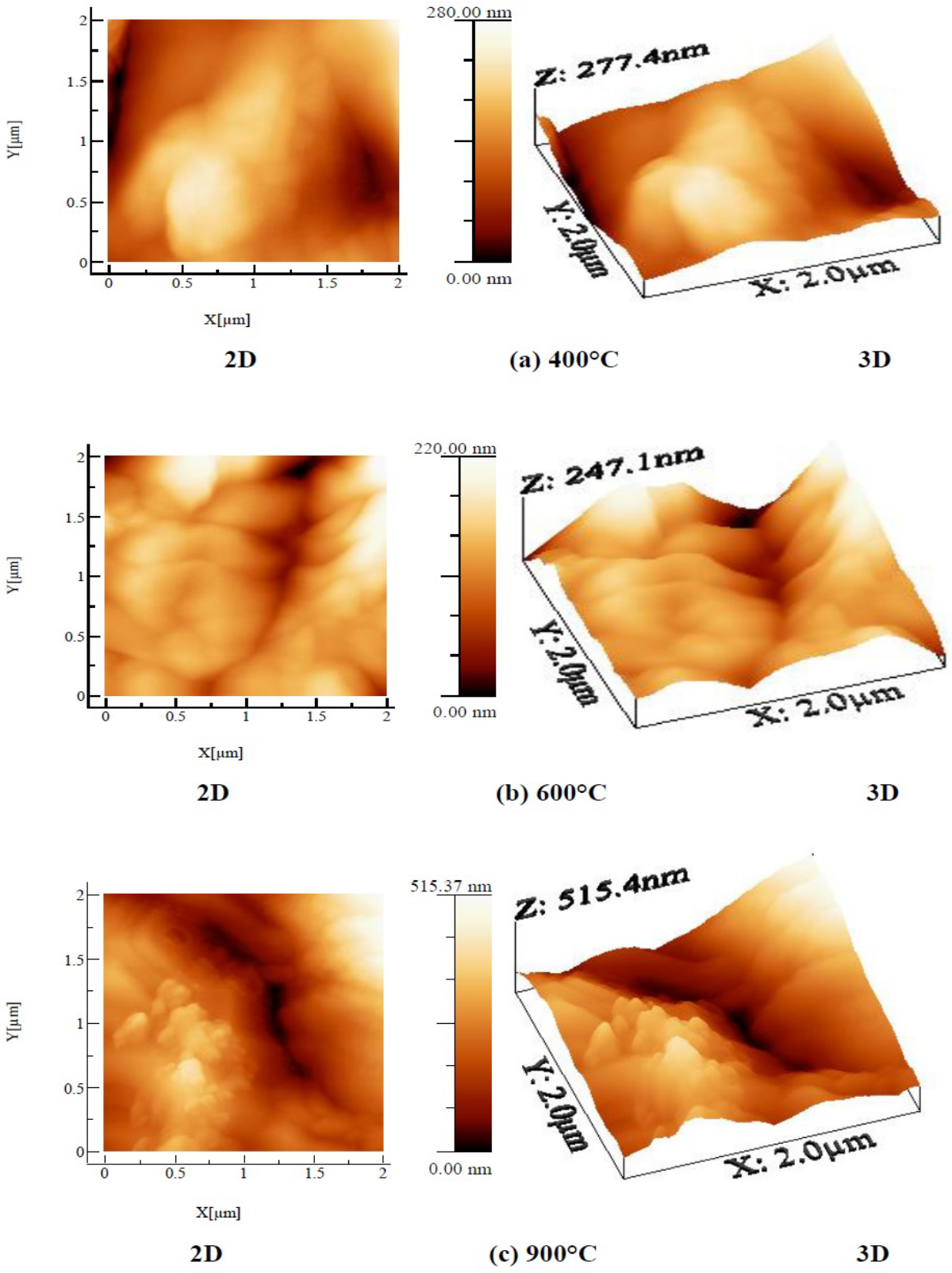

Figure 3: 2D and 3D AFM images (2 µm x 2 µm) of TiO_2 films on silicon substrates annealed at (a) 400°C, (b) 600°C, and (c) 900°C.

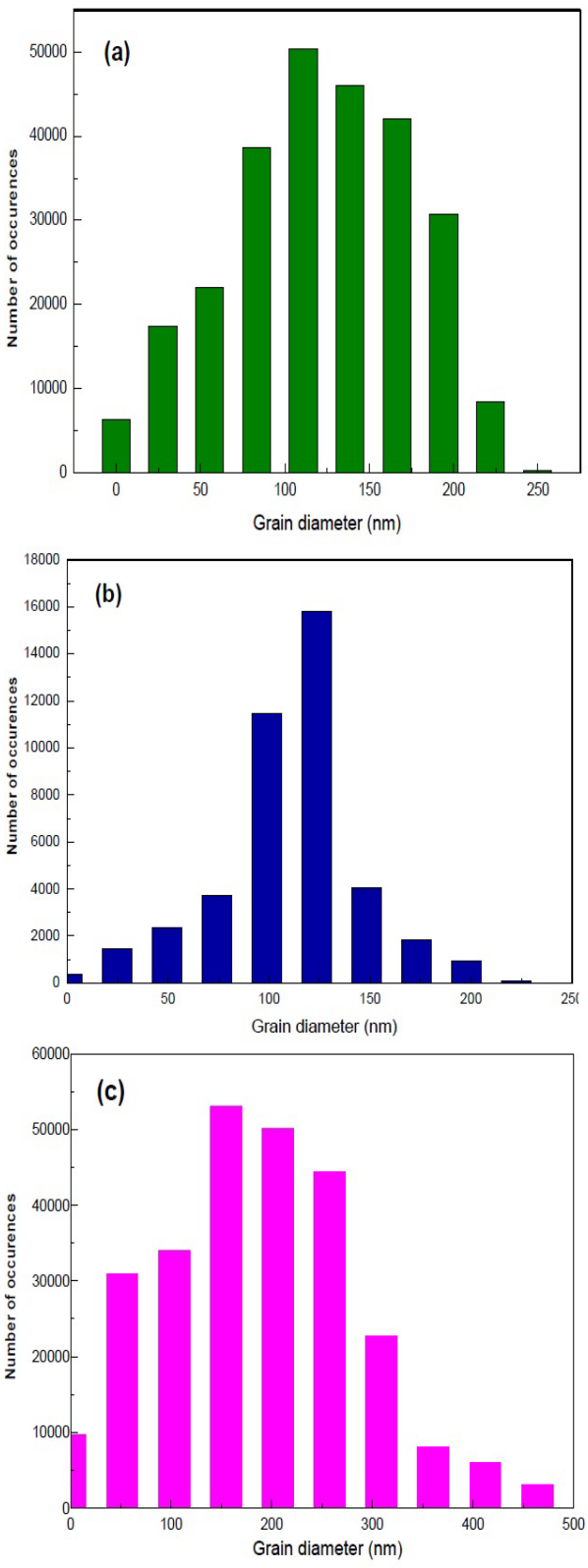

Figure 4: Grain size distribution of TiO_2 thin films on silicon substrates, annealed at (a) 400°C, (b) 600°C, and (c) 900°C, obtained from AFM measurements.

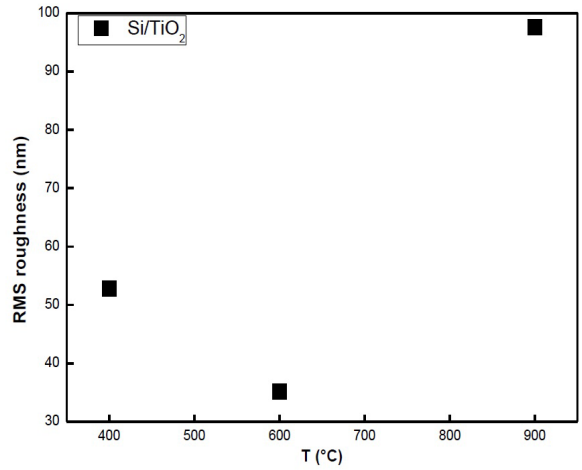

Figure 5: Surface roughness of TiO_2 films on silicon substrates, annealed at (a) 400°C, (b) 600°C, and (c) 900°C, obtained from AFM measurements.

annealed at 600°C and 700°C is observed. Moreover, for 600°C to 900°C the PL intensity for wavelengths shorter than 522 nm is lower than the intensity for longer wavelengths. This behavior is probably due to a mixed anatase-rutile phase. As shown in Figure 6, the PL spectra present a peak at 486 nm (2.55 eV) and a broad band around 585 nm (2.11 eV). The 585 nm band is attributed to the anatase phase and the 486 nm peak to the rutile phase [36]. The emission at 486 nm can be attributed to charge transfer from Ti^{3+} to the oxygen anion in a Tio_6^{8-} complex, associated with oxygen vacancies at the surface. There are three types of defects (oxygen vacancies, Ti^{4+} and Ti^{3+} interstitials), among which the formation of defects associated with Ti^{3+} is energetically more favorable. Therefore, this type of defect may be formed predominantly during the crystallization of anatase TiO_2, indicating this band originates from intrinsic rather than surface states [12,37]. As Chung et al. indicate, that, when the structure is a mixture of anatase and rutile phases at low oxygen flow ratio, additional electron states in the band gap are generated, which results in the occurrence of the 585 nm band [36]. In addition, a new radiative transition occurs, which leads to a new PL peak at 486 nm at the rutile phase, increasing with annealing temperature [38].

The 465 nm peak and the two overlapping peaks centered at 539 nm are attributed to defect states due to oxygen vacancies [12]. The PL intensity of these peaks decreases as the annealing temperature increases; this result indicates that oxygen vacancies disappear gradually with annealing temperature.

The phase transition (anatase to rutile) starts at 600°C and the mixed anatase-rutile phase appears at higher temperatures, as we can see by comparing the intensities of the two characteristics bands of anatase and rutile phases (585 nm and 486 nm, respectively). The intensity of the anatase band at 585 nm decreases and then gradually disappears for higher annealing temperatures, while the intensity of the rutile band at 486 nm still exists with annealing temperature, therefore we can speak about phase transition. In addition, the development of other broad bands around the 539 nm peak may indicate the presence of other shallow traps and defect states inside the band gap and mainly originate from the morphology distribution of the nanostructures [12].

Reflectivity: The reflectivity of the silicon substrate and TiO_2 films on silicon for different annealing temperatures has been measured in

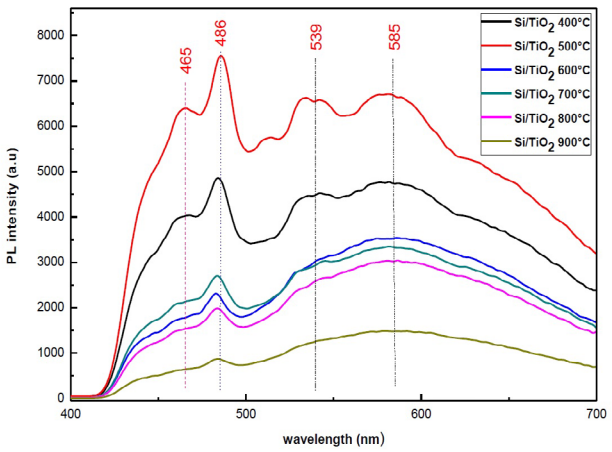

Figure 6: Room temperature PL spectra of TiO_2 thin films on silicon substrates annealed at different temperatures (400°C-900°C).

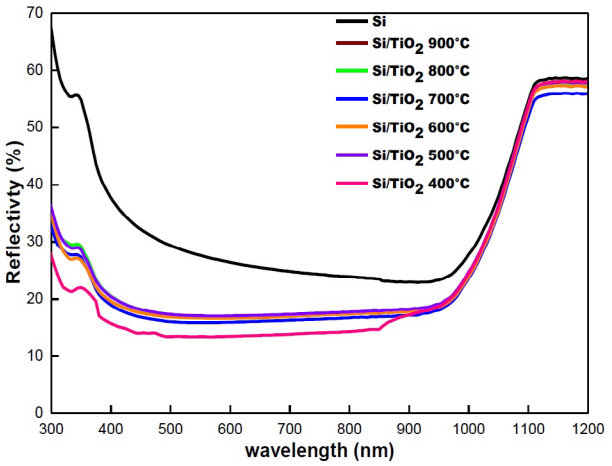

Figure 7: Reflectivity spectra of TiO_2 films, annealed at different temperatures (400°C-900°C).

the wavelength range from 300 to 1200 nm. Figure 7 indicates that the reflectivity of the films decreases from 37 to 13%, by comparing it with silicon reflectivity, in the region from 400 to 800 nm. The reduced reflectivity is usually explained by secondary reflections of the incident light at the sidewalls between grains. This reflectivity decrease indicates an efficient control of the antireflecting behavior of TiO_2 thin films [39,40].

Conclusions

Titanium oxide thin films were deposited on silicon substrates by using the sol-gel spin coating method and annealed at different temperatures (400°C-900°C). The Raman, AFM, and FTIR results indicate the dependence of the formed phases (anatase, rutile, or mixed anatase-rutile phase) of the TiO_2 films on the annealing temperature. The films annealed from 400°C to 900°C show the PL peaks at 486 nm (2.55 eV) according to rutile phase, while the 585 nm band (2.11 eV) confirms the presence of the anatase and disappears gradually for temperatures higher than 600°C. Furthermore, the deposition of TiO_2 thin films allows the control of the antireflecting properties of silicon substrate between 13% and 37% in the 400-800 nm region.

Acknowledgments

Part of this work has been done at National Hellenis Research Foundation. Theoretical and Physical Chemistry Institute, 48 Vasileos Konstantinou Ave., 11635 Athens, Greece and financed by the Tunisian Ministry of Higher Education and Scientific Research.

References

1. Elfanaoui A, Elhamri E, Boulkaddat L, Ihlal A, Bouabid K, et al. (2011) Optical and structural properties of TiO2 thin films prepared by sol–gel spin coating. International Journal of Hydrogen Energy 36: 4130-4133.
2. Carp O, Huisman CL, Reller A (2004) Photoinduced reactivity of titanium dioxide. Progress in Solid State Chemistry 32: 33-177.
3. O'regan B, Grätzel M (1991) A low-cost, high-efficiency solar cell based on dye-sensitized colloidal TiO 2 films. Nature 353: 737-740.
4. Zhang Y, Chen J, Xu C, Zhou K, Wang Z, et al. (2016) A novel photo-thermochemical cycle of water-splitting for hydrogen production based on TiO 2− x/TiO 2. International Journal of Hydrogen Energy 41: 2215-2221.
5. Xu S, Ng J, Zhang X, Bai H, Sun DD (2010) Fabrication and comparison of highly efficient Cu incorporated TiO 2 photocatalyst for hydrogen generation from water. International Journal of Hydrogen Energy 35: 5254-5261.
6. Sta I, Jlassi M, Hajji M, Boujmil MF, Jerbi R, et al. (2014) Structural and optical properties of TiO2 thin films prepared by spin coating. Journal of Sol-Gel Science and Technology 72: 421-427.
7. Al-Homoudi IA, Thakur JS, Naik R, Auner GW, Newaz G (2007) Anatase TiO 2 films based CO gas sensor: film thickness, substrate and temperature effects. Applied Surface Science 253: 8607-8614.
8. Chen TL, Furubayashi Y, Hirose Y, Hitosugi T, Shimada T, et al. (2007) Anatase phase stability and doping concentration dependent refractivity in codoped transparent conducting TiO2 films. Journal of Physics D: Applied Physics 40: 5961.
9. Das PP, Mohapatra SK, Misra M (2008) Photoelectrolysis of water using heterostructural composite of TiO2 nanotubes and nanoparticles. Journal of Physics D: Applied Physics 41: 245103.
10. Gräzel M (1989) Heterogeneous Chemical Electron Transfer. XRC Press Inc.
11. Serpone N, Lawless D, Khairutdinov R (1995) Size effects on the photophysical properties of colloidal anatase TiO2 particles: size quantization versus direct transitions in this indirect semiconductor?. The Journal of Physical Chemistry 99: 16646-16654.
12. Mathpal MC, Tripathi AK, Singh MK, Gairola SP, Pandey SN, et al. (2013) Effect of annealing temperature on Raman spectra of TiO 2 nanoparticles. Chemical Physics Letters 555: 182-186.
13. Rath C, Mohanty P, Pandey AC, Mishra NC (2009) Oxygen vacancy induced structural phase transformation in TiO2 nanoparticles. Journal of Physics D: Applied Physics 42: 205101.
14. Zhang H, Banfield JF (1999) New kinetic model for the nanocrystalline anatase-to-rutile transformation revealing rate dependence on number of particles. American Mineralogist 84: 528-535.
15. Mallak M, Bockmeyer M, Löbmann P (2007) Liquid phase deposition of TiO 2 on glass: systematic comparison to films prepared by sol–gel processing. Thin Solid Films 515: 8072-8077.
16. Hernández JL, Olmos JM, Alonso MA, González-Fernández CR, Martínez J, et al. (2006) Trend in hip fracture epidemiology over a 14-year period in a Spanish population. Osteoporosis International 17: 464-470.
17. Lin SS (2012) Effect of substrate temperature on the properties of TiO2 nanoceramic films. Ceramics International 38: 2461-2466.
18. Pradhan SS, Sahoo S, Pradhan SK (2010) Influence of annealing temperature on the structural, mechanical and wetting property of TiO 2 films deposited by RF magnetron sputtering. Thin Solid Films 518: 6904-6908.
19. Vyas S, Tiwary R, Shubham K, Chakrabarti P (2015) Study the target effect on the structural, surface and optical properties of TiO 2 thin film fabricated by RF sputtering method. Superlattices and Microstructures 80: 215-221.

20. Li D, Goullet A, Carette M, Granier A, Landesman JP (2016) Effect of growth interruptions on TiO 2 films deposited by plasma enhanced chemical vapour deposition. Materials Chemistry and Physics 182: 409-417.

21. Gotić M, Ivanda M, Sekulić A, Musić S, Popović S, et al. (1996) Microstructure of nanosized TiO2 obtained by sol-gel synthesis. Materials Letters 28: 225-229.

22. Pomoni K, Vomvas A, Todorova N, Giannakopoulou T, Mergia K, et al. (2011) Thermal treatment effect on structure, electrical conductivity and transient photoconductivity behavior of thiourea modified TiO 2 sol–gel thin films. Journal of Alloys and Compounds 509: 7253-7258.

23. Ibrahim NB, Al-Shomar SM, Ahmad SH (2013) Effect of aging time on the optical, structural and photoluminescence properties of nanocrystalline ZnO films prepared by a sol–gel method. Applied Surface Science 283: 599-602.

24. Ohsaka T (1980) Temperature dependence of the Raman spectrum in anatase TiO2. Journal of the Physical Society of Japan 48: 1661-1668.

25. Choi HC, Jung YM, Kim SB (2005) Size effects in the Raman spectra of TiO 2 nanoparticles. Vibrational Spectroscopy 37: 33-38.

26. Xu CY, Zhang PX, Yan L (2001) Blue shift of Raman peak from coated TiO2 nanoparticles. Journal of Raman Spectroscopy 32: 862-865.

27. Bezrodna T, Gavrilko T, Puchkovska G, Shimanovska V, Baran J, et al. (2002) Spectroscopic study of TiO 2 (rutile)–benzophenone heterogeneous systems. Journal of Molecular Structure 614: 315-324.

28. Mazza T, Barborini E, Piseri P, Milani P, Cattaneo D, et al. (2007) Raman spectroscopy characterization of Ti O 2 rutile nanocrystals. Physical Review B 75: 045416.

29. Wang X, Wu G, Zhou B, Shen J (2013) Optical constants of crystallized TiO2 coatings prepared by sol-gel process. Materials 6: 2819-2830.

30. Rabah B, Hanene B (2012) Heat treatment-Conventional and Novel Applications. INTECH, Chapter 10, pp: 207-234.

31. Nakamura R, Nakato Y (2004) Primary intermediates of oxygen photoevolution reaction on TiO2 (rutile) particles, revealed by in situ FTIR absorption and photoluminescence measurements. Journal of the American Chemical Society 126: 1290-1298.

32. Tripathi AK, Singh MK, Mathpal MC, Mishra SK, Agarwal A (2013) Study of structural transformation in TiO 2 nanoparticles and its optical properties. Journal of Alloys and Compounds 549: 114-120.

33. Zhao ZW, Tay BK (2006) Study of nanocrystal TiO 2 thin films by thermal annealing. Journal of Electroceramics 16: 489-493.

34. Pecharromán C, Gracía F, Holgado JP, Ocaña M, González-Elipe AR, et al. (2003) Determination of texture by infrared spectroscopy in titanium oxide–anatase thin films. Journal of Applied Physics 93: 4634-4645.

35. Ohsaka T, Izumi F, Fujiki Y (1978) Raman spectrum of anatase, TiO2. Journal of Raman Spectroscopy 7: 321-324.

36. Chung CK, Liao MW, Lai CW (2009) Effects of oxygen flow ratios and annealing temperatures on Raman and photoluminescence of titanium oxide thin films deposited by reactive magnetron sputtering. Thin Solid Films 518: 1415-1418.

37. Saraf LV, Patil SI, Ogale SB, Sainkar SR, Kshirsager ST (1998) Synthesis of nanophase TiO 2 by ion beam sputtering and cold condensation technique. International Journal of Modern Physics B 12: 2635-2647.

38. Jin C, Liu B, Lei Z, Sun J (2015) Structure and photoluminescence of the TiO 2 films grown by atomic layer deposition using tetrakis-dimethylamino titanium and ozone. Nanoscale Research Letters 10: 95.

39. Jannat A, Lee W, Akhtar MS, Li ZY, Yang OB (2016) Low cost sol–gel derived SiC–SiO 2 nanocomposite as anti reflection layer for enhanced performance of crystalline silicon solar cells. Applied Surface Science 369: 545-551.

40. López G, Ortega PR, Voz C, Martín I, Colina M, et al. (2013) Surface passivation and optical characterization of Al2O3/a-SiCx stacks on c-Si substrates. Beilstein Journal of Nanotechnology 4: 726.